CrystEngComm

Accepted Manuscript

This is an *Accepted Manuscript*, which has been through the Royal Society of Chemistry peer review process and has been accepted for publication.

Accepted Manuscripts are published online shortly after acceptance, before technical editing, formatting and proof reading. Using this free service, authors can make their results available to the community, in citable form, before we publish the edited article. We will replace this *Accepted Manuscript* with the edited and formatted *Advance Article* as soon as it is available.

You can find more information about *Accepted Manuscripts* in the Information for Authors.

Please note that technical editing may introduce minor changes to the text and/or graphics, which may alter content. The journal's standard Terms & Conditions and the Ethical guidelines still apply. In no event shall the Royal Society of Chemistry be held responsible for any errors or omissions in this *Accepted Manuscript* or any consequences arising from the use of any information it contains.

ROYAL SOCIETY OF CHEMISTRY

www.rsc.org/crystengcomm

One-step hydrothermal synthesis of cobalt and potassium codoped CdSe quantum dots with high visible light photocatalytic activity

Changchang Ma, Mingjun Zhou, Dan Wu, Mengyao Feng, Xinlin Liu, Pengwei Huo, Weidong Shi*, Zhongfei Ma, Yongsheng Yan*

The effect of metal ions doping on the electronic structure and optical properties of CdSe quantum dots have been investigated by the various characterization and experiment. Various cation codoped CdSe quantum dots photocatalysts were synthesized via a hydrothermal method. The prepared quantum dots were examined using X-ray diffraction, fluorescence spectroscopy, X-ray photoelectron Spectroscopy, high resolution transmission electron microscopy, and UV–vis diffuse reflectance spectroscopy. The activities of the photocatalysts were evaluated in photodegradation of tetracycline hydrochloride solutions under simulated sunlight irradiations. 3%Co-4%K/CdSe quantum dots showed a higher photocatalytic activity within 30 min under visible irradiation than others. Furthermore, there was hardly decrease of catalytic efficiency after the fourth experiment. Identification data illustrate that Co and K codoping may cause the improvement of the photocatalytic performance of CdSe quantum dots, which is crucial to tetracycline hydrochloride degradation under simulated sunlight irradiations. Therefore this study demonstrated a promising strategy for design of highly efficient photocatalysts for remediation of aqueous pollutants.

Keywords: CdSe; quantum dots; photocatalytic degradation; tetracycline hydrochloride; codope

1. Introduction

Antibiotics are among the emerging microcontaminants in water because of concerns of their

School of Environment and Safety Engineering, Jiangsu University, Zhenjiang 212013, China
E-mail: machang719@126.com; Fax: +86 511 88791108;
Tel: +86 511 88790187

CrystEngComm Accepted Manuscript

potential adverse effects on the ecosystem and possibly on human health. Antibiotics are likely to be released into the aquatic environment via wastewater effluent and agricultural run off as a result of incomplete metabolism, ineffective treatment removal or improper disposal because large quantities of antibiotics are used annually in human therapy and in agriculture [1-5]. Among all the antibiotics, tetracycline hydrochloride is extensively used for disease control due to their great therapeutic values. Furthermore, the residues of tetracycline hydrochloride have potential threaten to human. Therefore, it is necessary to treat and dispose the residues of tetracycline hydrochloride in the waste water [6].

In order to solve this problem, it is necessary to introduce an effective method. Photocatalytic technology, as a prospective method, exhibits a high efficiency in oxidizing some organic compounds with high degradation ratios and of low cost [7-10]. Recently, some studies on the photodegradation of antibiotics have been reported, but there is little report on photocatalysis using quantum dots (QDs) as a photocatalyst.

Quantum dot materials have already attracted a great deal of scholars' interest due to unique original optical and electronic characters. The photogenerated electron–hole pairs and their subsequent split up into free carriers are the two key elements which directly determine the light response efficiency of the quantum dots materials [11-12]. CdSe is a conventional II-IV semiconductor quantum dot with a gap band of 1.7eV that can play the part of an excellent photocatalytic material [13-15]. However, the CdSe quantum dots also have some shortcomings, such as photocorrosion or photodissolution, which severely restricts its photocatalytic properties and reduces its stability [16-18]. Hence, it is necessary for us to take steps to overcome its drawbacks. Fortunately, the defects of the CdSe quantum dots can be improved by further

CrystEngComm Accepted Manuscript

modification via loading [19-22], doping [23-26] and so on.

In the past few years, a great deal of work has been focused on altering the lattice structure and enhancing the stability of CdSe quantum dots. For instance, the materials were doped by transition metals such as Zn, Co, Mn, and Cu, in order to change the lattice structure of CdSe quantum dots [27-29]. Nevertheless, the shortcomings of materials doped by transition metal are ascribed their poor thermostability, generated recombination centers of electrons and holes and the strict demand of instruments. Some of the newest studies suggest that the band gap of CdSe could be further narrowed by codoping various ions and the photocatalytic activity also could be improved [30-31].

In this study, the effect of different metal ions codoping concentration and variety on the photocatalytic activity was studied. The molar ratio of Co/K = 3:4 CdSe quantum dots have the best photocatalytic activity on degradation of tetracycline hydrochloride under visible-light irradiation. The tentative mechanism of photocatalytic reaction on K and Co-codoped CdSe quantum dots was also discussed based on our experimental results and our understanding.

2. Experiment selection

2.1 materials

All chemicals used in the study were analytical grade without further treatment. Cadmium chloride hemi(pentahydrate), cobalt chloride hexahydrate, zinc chloride, calcium chloride, kalium chloride, iron chloride hexahydrate, tetracycline hydrochloride, sodium dodecyl sulfate, tert-Butanol, edetate disodium, sodium hydroxide, hydrochloric acid were purchased from Shanghai Guoyao Chemical Co. Se power, sodium borohydride, 3-mercaptopropionic acid, polyethylene glycol 2000, benzalkonium chloride were purchased from aladdin.

CrystEngComm Accepted Manuscript

2.2 Samples preparation

The synthesis of metal doped CdSe quantum dots was carried out by a simple hydrothermal method. In the typical synthesis procedure, 0.4mmol cadmium chloride hemi(pentahydrate) was dissolved in de-ionized water. 3-mercaptopropionic acid was used as a capping agent. Further, 0.75mmol selenium (Se) was reduced with sodium borohydride and this solution was added into the cadmium chloride hemi (pentahydrate) solution. Finally, the mixture was transferred to 50 ml Teflon-lined autoclave. The autoclave was then placed for 40min at 160 °C in oven. After that, the precipitates were washed first with distilled water, then with ethanol for several times, and dried in hot air oven under the ambient conditions to obtain the powder. After being cooled down to room temperature naturally, the products were precipitated through centrifugation, washed for 3 times by distilled water and absolute alcohol, and dried at 60 ^{o}C for 12h. In order to obtain different products, the experimental parameters, such as the kind of metal ions, the amount of metal ion had been changed during the synthesis.

2.3 Characterization

Transmission electron microscopy (TEM) images were collected on a JEM 2100 (JEOL, Japan), using a 100 kV accelerating voltage. Powder X-ray diffraction (XRD) patterns were obtained with an X'pert PROMPD diffractometer (PANalytical, Holland) with copper Kα1 radiation at a scan rate of 5° min.1 to determine the crystal phase of these samples. UV–vis absorption spectroscopies of the samples were obtained from a UV–vis spectrophotometer (Shimadzu UV2450, Japan) equippedwith an integrating sphere. BaSO4 was used as a reflectance standard. X-ray photoelectron spectroscopy (XPS) data were collected on a PHI5300 analyzer (Perkin Elmer, USA) with aluminum Kα radiation. The intermediates produced during the

CrystEngComm Accepted Manuscript

degradation of tetracycline hydrochloride were monitored using HPLC-MS (Shimadzu HPLC-2010A system) equipped with a C-18 column. The photoluminescence (PL) spectra were recorded by a Hitachi F-4500 fluorescence spectrophotometer with a Xe lamp as the excitation source.

2.4 Photocatalysis experiment

The photocatalysis experiment of tetracycline hydrochloride solution was implemented in self-made photocatalytic equipment under visible light. A 500W Xe lamp served as a visible light source with an ultraviolet cutoff filter, which offers possibility for the permeance of visible light with wavelengths longer than 420nm ($\lambda > 420$nm). During the experiment, 0.05g of photocatalyst was added into 100mL tetracycline hydrochloride solution with a concentration of 20mg L^{-1}. As the role of recycling water, the temperature of the tetracycline hydrochloride was kept about 30 ± 0.5°C during the photocatalytic process. In order to ensure the establishment of an adsorption/desorption equilibrium, the tetracycline hydrochloride solution was stirred in the dark for 10min. At 5min intervals of irradiation, roughly 4mL of the solution was separated and centrifuged to remove the solid catalysts. The concentrations of the tetracycline hydrochloride were measured with a UV–Vis spectrophotometer (Shimadzu UV2450, Japan) by checking the absorbance at 357nm.

3. Results and discussion

3.1 Phase structures

The XRD patterns of the undoped CdSe quantum dots and doped CdSe quantum dots are displayed in Fig. 1. The diffraction pattern displayed three different peaks: the peak at a diffraction angle of 2θ values 25.48° is ascribed to the (111) reflection and the two broad peaks located at 2θ

CrystEngComm Accepted Manuscript

values 42.21°and 49.96° are in line with (220) and (311) reflections. Referring to the standard data of JCPDS card No.65-2891, the lattice constant were marked as a=6.050 b=6.050 and c=6.050Å, which indicates the prepared undoped CdSe quantum dots are cubic structure. Compared with the diffraction curve of undoped CdSe quantum dots, the diffraction peaks of the doped CdSe quantum dots show a slight change to higher 2θ value, which demonstrates the metal ions have been doped to lattice and then remained cubic structure. The quantum dots sizes calculated from the broadening of (111) diffraction peak according to Debye–Scherrer's formula

$$D=k\lambda /\beta\cos\theta$$

Where, D is the grain size, K is a const taken to be 0.94, λ is the wavelength of X-ray, β is the full width at half maximum of the diffraction peak and θ is scattering angle. It can be concluded from the diffraction curves of the K-Co codoped CdSe quantum dots that the estimated particle size was within the scope of 8-9nm.

3.2 Morphology

The TEM and HR-TEM results of the prepared 3%Co-4%K/CdSe quantum dots heated at 160°C for 40min are shown in Fig. 2. As shown in the TEM micrograph that the nanoparticles are uniform, global and slightly agglomerated and the average particle size of 8nm estimated as an average of the measured size of a great deal of particles that could be exactly recognized on each exhibition that is in conformity with the XRD measurement of particle size. Fig. 2(B) shows the HR-TEM of the prepared 3%Co-4%K/CdSe quantum dots, which demonstrates that quantum dots contain a well-crystallized lattice.

3.3 Chemical states of surface elements

The valence and composition of elements of the K-Co-CdSe quantum dots was testified by

CrystEngComm Accepted Manuscript

the XPS spectra of the K-Co-CdSe quantum dots. A wide-ranging XPS spectrum of K-Co-CdSe quantum dots is illustrated as in Fig. 3A. Above all, the curve exhibit dramatic O1s and C1s peaks at 533 and 289eV, perhaps due to the surface of sample was covered by organic capping agent. Moreover, the presence of other substances was not detected. As you can see in Fig. 3B, the Co2p XPS spectra of the spinel cobaltite consists of two main lines with the $Co2p_{3/2}$ at a binding energy of 781.91eV and the $Co2p_{1/2}$ at 795.48eV with the spin-orbit splitting of 13.57eV, which are aligned with literature [26], indicating that cobalt mainly exists Co^{3+}[26]. The binding energies of Cd3d core levels for the samples situate in 403.8 and 411.28eV for $3d_{5/2}$ and $3d_{3/2}$, respectively (Fig. 3C), which suggests that Cd is in 2+ oxidation state. With regard to CdSe quantum dots, the Se3d (Fig. 3D) region shows the peak around 53.31eV is corresponding to the Se3d, which reveals the existence of Se^{2-} ion.

3.4 Optical absorption properties

In this research, the UV-vis absorption spectra were used to observe adsorption edge and energy band structures of metal ion doped CdSe quantum dots. In Fig. 4(A), all of the samples demonstrated excellent visible-light absorption from 658 to 720nm. For a crystalline semiconductor, it shown that the optical absorption near the band edge follows the equation $ah\upsilon=A(h\upsilon-E_g)$, where a, V, Eg, and A are the absorption coefficient, the light frequency, the band gap, and a constant, respectively. The relationship between $(\alpha h\nu)^2$ and energy of undoped and doped CdSe quantum dots was illustrated as in Fig. 4(B). The undoped CdSe quantum dot has a band gap of 1.6eV and doped CdSe quantum dot has a band gap of 1.75eV [27]. Compared with the undoped CdSe, the absorption spectrum of Co/K-doped quantum dots shows an obvious redshift trend. Due to the narrow band gap, the Co/K-doped quantum dots photocatalyst could

CrystEngComm Accepted Manuscript

generate more excited electron and hole when irradiated with visible light. Over the course of ion doping,

3.5 Photoluminescence properties

As everyone knows, the PL emission has a close relationship with the recombination of excited electrons and holes. Weaker PL intensity caused by the lesser recombination of excited electrons and holes in the field of optics. The PL spectra of pure CdSe quantum dots and CdSe quantum dots doped with different metal ions were shown in Fig. 5. As can be watched from the picture, the PL intensity of K and Co-codoped CdSe quantum dots is lowest among the four samples. All results above indicated that the K and Co-codoped CdSe quantum dots are the best photocatalyst, compared to the others.

3.6 Degradation of Tetracycline hydrochloride

3.6.1 Effect of dopants on the photocatalytic activity

The photocatalytic activity of the undoped and doped CdSe quantum dots were evaluated by monitoring the degradation of tetracycline hydrochloride. As shown in Fig. 6, the “Dark environment” shows the concentration of tetracycline hydrochloride almost keeps the same from 10 to 30minutes using catalysts without the visible-light irradiation, it indicates that the adsorption equilibrium of tetracycline hydrochloride onto the photocatalyst was achieved in 10min. The ‘Blank’ shows that tetracycline hydrochloride almost cannot be degraded under the visible-light irradiation without catalysts, indicating that the photolysis can be ignored. The doped CdSe quantum dots present the better photocatalytic activity than pure CdSe quantum dots, especially K and Co-codoped CdSe quantum dots. For K and Co-codoped CdSe quantum dots (see Fig. 4), it has the best photocatalytic activity compared with the K-, Co-doped CdSe quantum dots, which is

CrystEngComm Accepted Manuscript

due to the enhanced optical absorption of visible and UV-light through K and Co codoping. Therefore, the K and Co-codoped CdSe quantum dots exhibits best photocatalytic activity than K-, Co-doped CdSe quantum dots. The photocatalytic activity of prepared samples has following sequence: K and Co-codoped CdSe quantum dots > Co-doped CdSe quantum dots > K-doped CdSe quantum dots > pure CdSe quantum dots. Additionally, the photocatalytic ability of the K and Co-codoped CdSe quantum dots was compared with the reported works and the result was shown in table S1.

3.6.2 Effect of kind of metal ions on the photocatalytic activity

In the Fig. 7, the effect of different metal ions doping on the photocatalytic degradation of tetracycline hydrochloride was carried out at the initial concentration of 20mg/L. It can be observed that the samples doped with appropriate amount of Co ion and K ion had much higher photocatalytic activity compared with others, especially the sample with the molar ratio of Co/K = 3:4, which exhibited the best photocatalytic activity. Co^{2+} and K^{+} dopant can serve as charge traps retarding electron–hole combination rate and thereafter enhancing the interfacial charge transfer for tetracycline hydrochloride degradation within a suitable molar ratio of Co/K.

3.6.3 The photocatalytic effect of doped proportions of cobalt ions

In the Fig. 8, the effect of different doped proportions of cobalt ions on the photocatalytic degradation of tetracycline hydrochloride was carried out at the initial concentration of 20mg/L. As we all know, there are many factors that can improve the visible-light activity of codoped samples and the most important of which is the reduction of recombination of electron and holes. The Co^{3+}/Co^{2+} pair exists on the surface of solid catalysts while playing the part of electron traps. The Co^{3+} could capture excited electron, when the photocatalyst was exposed to visible light. In

CrystEngComm Accepted Manuscript

the meantime, the electrons provided by the hydroxyl groups combined with the residual holes (h^+), and eventually result in generating hydroxyl radicals ($^{\bullet}OH$), as the following eqs 1-2 show.

$$h^+ + H_2O \rightarrow HO^{\cdot} + H^+ \quad (1)$$

$$HO^{\cdot} + \text{antibiotic} \rightarrow \text{degradation} \quad (2)$$

The electrons that were captured by Co^{3+} could be move to the oxygen dissolved in water as well as be in charge of to degrading the antibiotics as the following eqs 3-5 show.

$$Co^{3+} + e^- \rightarrow Co^{2+} \quad (3)$$

$$Co^{2+} + O_2 \rightarrow O_2^{\cdot} + Co^{3+} \quad (4)$$

$$O_2^{\cdot -} + \text{antibiotic} \rightarrow \text{degradation} \quad (5)$$

Consequently, the existence of the Co^{3+}/Co^{2+} pair can efficiently prevent the recombination between electrons and holes as well as affect the removal efficiency of the tetracycline hydrochloride. As shown in Fig. 8, 3%Co-4%K/CdSe quantum dots exhibit the highest photocatalytic activity. This may be due to when the doping concentration of the Co far more than 3%Co-4%K/CdSe quantum dots, and then the surface and internal of pholocatalyst will generate defects that play the role of the recombination centers of the carriers.

3.6.4 The photocatalytic effect of surfactants

The influence of different surfactants on the catalytic performance was investigated in the following experiment. As shown in Fig. 9, Adding benzalkonium chloride which is a kind of cationic surfactant to solution, the best degradation rate was achieved. Due to when cationic surfactant ionizes in water, there is a lot of positive charge on its surface. Compared electronics with holes, holes play a dominant role in photodegradation. Due to the cationic surfactant ionize in the water, a large number of electrons are adsorbed onto the surface of the surfactant. Then a great

CrystEngComm Accepted Manuscript

deal of holes would be released as free holes and participated in visible light catalytic reaction, improving the photocatalytic performance of catalyst. Furthermore, the presence of the cationic surfactant can effectively inhibit the recombination of electrons and holes which can some extent promote the activity of the catalyst.

3.6.5 Mechanism of Photocatalysis

It is significant to understand the major reactive radicals in the photocatalytic reaction for mastering the photodegradation mechanism. The major reactive radicals in photodegradation could be tested by the trapping experiments, such as hydroxyl radical, superoxide radical, electrons and holes [30]. The photodegradation of tetracycline hydrochloride with the addition of tert-butyl alcohol (t-BuOH), benzoquinone, methanol and disodium ethylenediamine tetraacetate (EDTA-Na) was demonstrated in Fig. 10. The addition of t-BuOH as a capture of hydroxyl radical obtained a higher photodegradation efficiency of tetracycline hydrochloride, while tetracycline hydrochloride was hardly degraded with the addition of the holes scavenger (EDTA-Na) and only a small fraction was degraded when the existence of electrons scavenger (methanol) and superoxide radical scavenger (benzoquinone). All results above indicated that holes were the major reactive radicals of the tetracycline hydrochloride degradation as well as the electrons and superoxide radical play a certain role in degradation of tetracycline hydrochloride [31-32].

3.7 The process of degradation

It was important to investigate the direct detection of reactive intermediates in the photocatalytic system of tetracycline hydrochloride degradation mechanism. HPLC-MS was applied accurately to identify the intermediates. The results are illustrated as in Fig. 11. As can be watched from Fig. 11(A), a strong remarkable ion with m/z = 445 was the deprotonated

CrystEngComm Accepted Manuscript

tetracycline hydrochloride molecular ion and the peaks of their main intermediates were detected. Based on the analysis of MS, the hydroxy radical as the strong oxidant, attacked the tetracycline hydrochloride, and replaced the H of tetracycline hydrochloride, then obtain m/z = 475. The following order was limited by consecutive ions attacked and their fragment upon collision-induced dissociation: m/z = 445 → m/z = 362 → m/z = 318→ m/z =302 → m/z =274. The process of the photodegradation was displayed in Fig. 12. At last, the byproducts would be decomposed to the small molecular material.

3.8 Photocatalytic mechanism

The possible mechanism that the photocatalytic degradation performance of CdSe quantum dots are enhanced by doped metal ions is advanced in Fig. 13. As a result of cobalt ions doping, a new condition which could make energy gap narrow has formed. In the event, separation of electrons and holes gets easier. The excited electrons moved to oxygen molecules that are adsorbed onto the solid catalysts to generate free radicals, such as O_2^-, $\bullet HO_2$ and so on. The photoinduced holes and free radicals play the key role in degrading targets.

3.8 The stability of the photocatalyst

As the indispensable important parameter in appraising of photocatalytic ability, stability has significant influence on its application. The repeated experiments for the degradation of tetracycline hydrochloride using the 0.05wt% K-Co-CdSe quantum dot photocatalysts were carried out to estimate its stability. The repeated experiments for the degradation of tetracycline hydrochloride were shown in Fig. 14, and there was almost unchanged of catalytic efficiency after the fourth experiment. Consequently, the K-Co-CdSe quantum dots can take the role of the stable photocatalysts in practical application. In addition, the elemental speciation of the photocatalyst

CrystEngComm Accepted Manuscript

before and after degradation of tetracycline hydrochloride was displayed in Figure 15. It shows that the position of diffraction peaks was nearly no change. But the intensity of O1s and C1s peaks were obviously enhanced, this may be due to a large number of oxygen-containing groups were produced on the surface of the catalyst as well as some tetracycline hydrochloride was also adsorbed on catalyst surface.

4. Conclusions

The K-Co codoped CdSe quantum dots have been successfully prepared by one-step hydrothermal process. Compared with other samples, the molar ratio of K/Co = 4:3 CdSe quantum dots have the better photocatalytic efficiency for the removal of tetracycline hydrochloride in visible light irradiation. Beyond that, the K-Co codoped CdSe quantum dots have superior recycle property, as the removal efficiency stayed the same in virtually over the next four recycle. An appropriate proportion of K and Co embedded into CdSe lattice could bring about the change of the energy gap of CdSe to the aspects with easily being excited. Moreover, the excellent photocatalytic ability of the K-Co codoped CdSe quantum dots makes a contribution to be used to degrade toxic pollutants from sewage. The one step hydrothermal processes without other organic solvents provide an environmentally friendly approach for materials synthesis.

Acknowledgements

This work was financially supported by the Natural Science Foundation of Jiangsu Province (No.BK20131259 No.BK20130489), the Ph.D. Programs Foundation of Ministry of Education of China (No.20113227110019), and the Natural Science Foundation of China (No.21207053).

CrystEngComm Accepted Manuscript

References

[1]. A. Pruden, Environ. Sci. Technol. 2014, 48, 5-14.

[2]. B. W. Chen, Y. Yang, X. M. Liang, K Yu, T Zhang, X. D. Li, Environ. Sci. Technol. 2013, 47, 12753-12760.

[3]. X. H. Wang, Y. C. Lin, Environ. Sci. Technol. 2012, 46, 12417-12426.

[4]. P. Heneberg, J. Chem. Inf. Model. 2011, 51, 1-2.

[5]. L. Ge, J. W. Chen, X. X. Wei, S. Y. Zhang, X. L. Qiao, X. Y. Cai, Q. Xie, Environ. Sci. Technol. 2010, 44, 2400-2405.

[6]. S. Kim, P. Eichhorn, J. N. Jensen, A. S. Weber, D. S. Aga, Environ. Sci. Technol. 2005, 39, 5816-5823.

[7]. O. S. Keen, K. G. Linden, Environ. Sci. Technol. 2013, 47, 13020-13030.

[8]. Z. Y. Lu, Y. Y. Luo, M. He, P. W. Huo, T. T. Chen, W. D. Shi, Y. S. Yan, J. M. Pan, Z. F. Ma, S. Y. Yang, RSC Adv. 2013, 3, 18373-18382.

[9]. X. L. Liu, P. Lv, G. X. Yao, C. C. Ma, P. W. Huo, Y. S. Yan, Chem. Eng. J. 2013, 217, 398-406.

[10]. Y. Liu, M. J. Zhou, Y. Hu, H. S. Qian, J. F. Chen, X. Hu, CrystEngComm 2012, 14, 4507-4512.

[11]. N. Akopian, G. Patriarche, L. Liu, J. C. Harmand, V. Zwiller, Nano Lett. 2010, 10, 1198-1201.

[12]. S. W. Clark, J. M. Harbold, F. W. Wise, J. Phys. Chem. C 2007, 111, 7302-7305.

[13]. K. B. Subila, G. K. Kumar, S. M. Shivaprasad, K. G. Thomas, J. Phys. Chem. Lett. 2013, 4, 2774-2779.

[14]. X. L. Liu, C. C. Ma, Y. Yan, G. X. Yao, Y. F. Tang, P. W. Huo, W. D. Shi, Y. S. Yan, Ind. Eng. Chem. Res. 2013, 52, 15015-15023.

[15]. A. Thibert, F. A. Frame, E. Busby, M. A. Holmes, F. E. Osterloh, D. S. Larsen, J. Phys. Chem. Lett. 2011, 2, 2688-2694.

[16]. P. J. Cameron, X. H. Zhong, W. Knoll, J. Phys. Chem. C 2009, 113, 6003-6008.

[17]. K. Tvrdy, P. V. Kamat, J. Phys. Chem. A 2009, 113, 3765-3772.

[18]. J. Zhao, M. A. Holmes, F. E. Osterloh, ACS Nano 2013, 7, 4316-4325.

[19]. S. L. Cheng, W. Y. Fu, H. B. Yang, L. N. Zhang, J. W. Ma, H. Zhao, M. L. Sun, L. H. Yang, J. Phys. Chem. C 2012, 116, 2615-2621.

[20]. J. Hensel, G. M. Wang, Y. Li, J. Z. Zhang, Nano Lett. 2010, 10, 478-483.

[21]. L. Jia, D. H. Wang, Y. X. Huang, A. W. Xu, H. Q. Yu, J. Phys. Chem. C 2011, 115, 11466-11473.

[22]. Y. L. Lee, C. F. Chi, S. Y. Liau, Chem. Mater. 2010, 22, 922-927.

[23]. L. G. Gutsev, N. S. Dalal, G. L. Gutsev, Comp. Mater. Sci. 2014, 83, 261-268.

[24]. R. W. Meulenberg, T. V. Buuren, K. M. Hanif, T. M. Willey, G. F. Strouse, L. J. Terminello, Nano Lett. 2004, 4, 2277-2285.

[25]. J. Jasinski, J. Phys. Chem. C 2009, 113, 13008-13015.

[26]. Y. M. Sung, W. C. Kwak, T. G. Kim, Cryst. Growth. Des. 2008, 8, 1186-1190.

[27]. S. Arif, B. Amin, Iftikhar Ahmad, M. Maqbool, R. Ahmadc, M. Haneef , N. Ikrama, Curr. Appl. Phys. 2012, 12, 184-187.

[28]. P. I. Archer, S. A. Santangelo, D. R. Gamelin, Nano Lett. 2007, 7, 1037-1043.

[29]. L. J. Hill, N. E. Richey, Y. Sung, P. T. Dirlam, J. J. Griebel, I. Shim, N. Pinna, M. Willinger,

CrystEngComm Accepted Manuscript

W. Vogel, K. Char, J. Pyun, CrystEngComm 2012, 16, 9461-9468.
[30]. M. Nasir, Z. H. Xi, M. Y. Xing, J. L. Zhang, F. Chen, B. Z. Tian, S. Bagwasi, J. Phys. Chem. C 2013, 117, 9520-9528.
[31]. T. G. Xu, L. W. Zhang, H. Y. Cheng, Y. F. Zhu, Appl. Catal. B-Environ. 2011, 101, 382-387.
[32]. A. Huang, N. Wang, M. Lei, L. H. Zhu, Y. Y. Zhang, Z. F. Lin, D. Q. Yin, H. Q. Tang, Environ. Sci. Technol. 2013, 47, 518-525.
[33]. X. J. Bai, L. Wang, Y. F. Zhu, ACS Catal. 2012, 2, 2769-2778.

CrystEngComm Accepted Manuscript

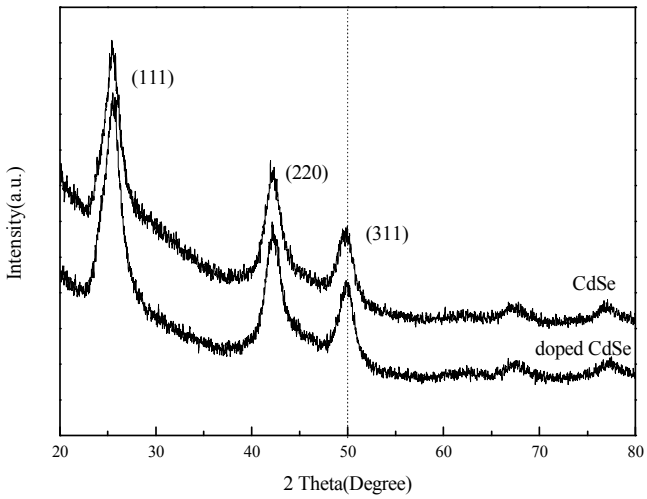

Fig. 1

CrystEngComm Accepted Manuscript

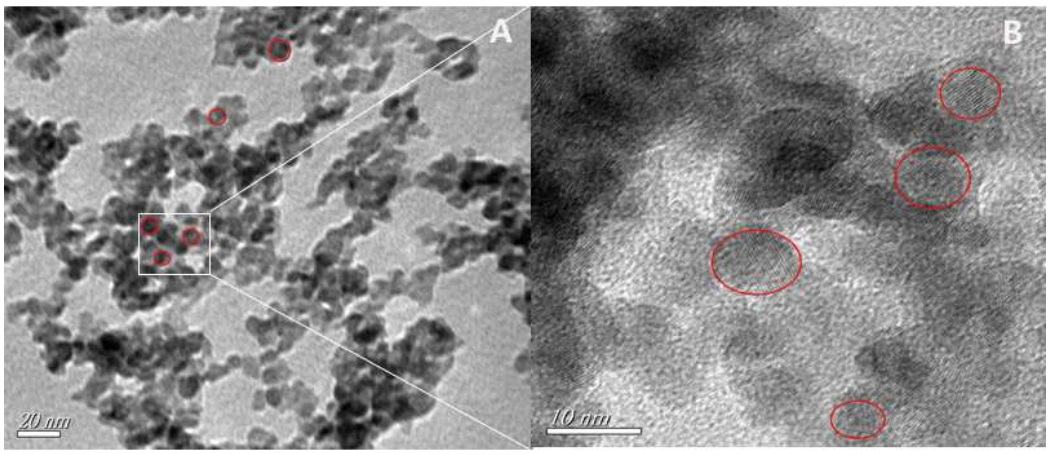

Fig. 2

CrystEngComm Accepted Manuscript

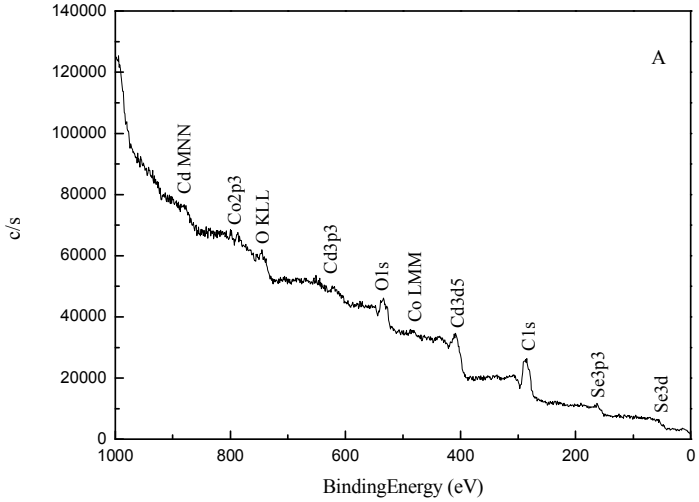

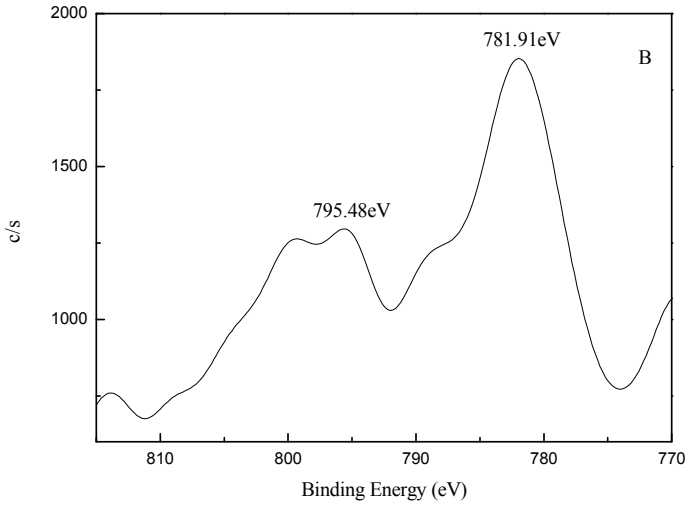

CrystEngComm Accepted Manuscript

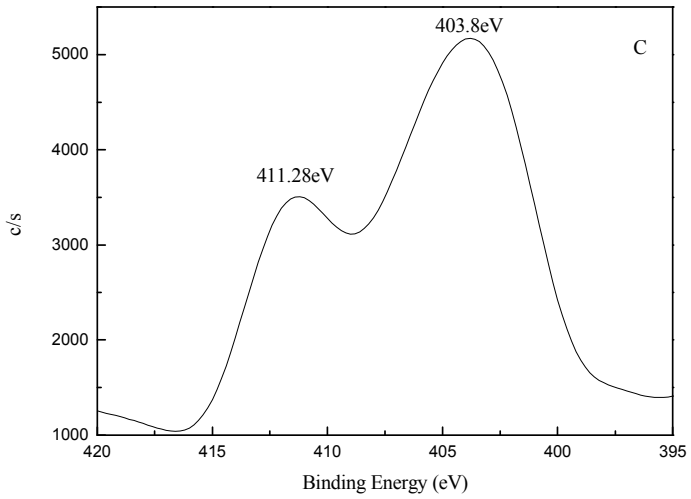

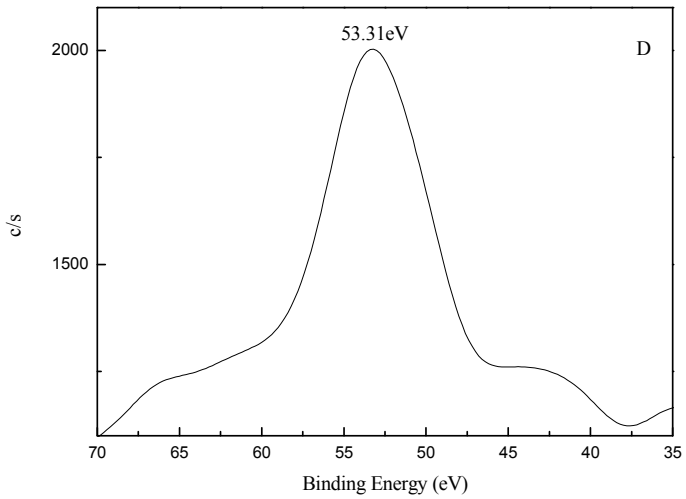

Fig. 3

CrystEngComm Accepted Manuscript

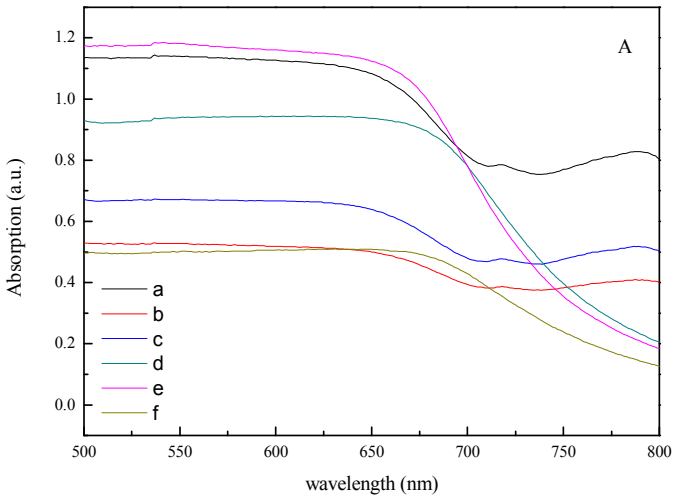

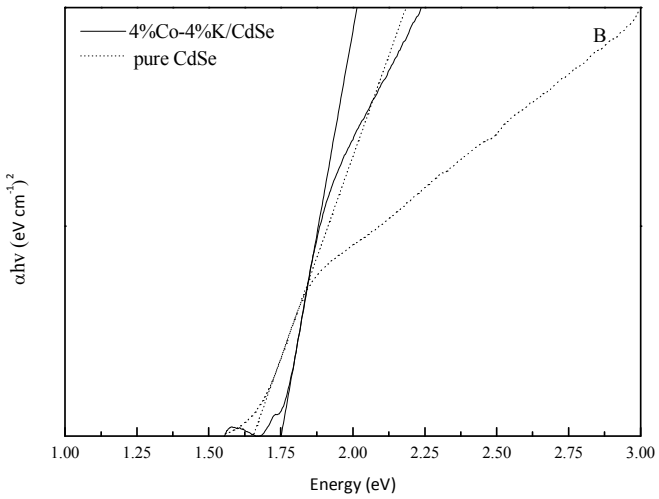

Fig.4

CrystEngComm Accepted Manuscript

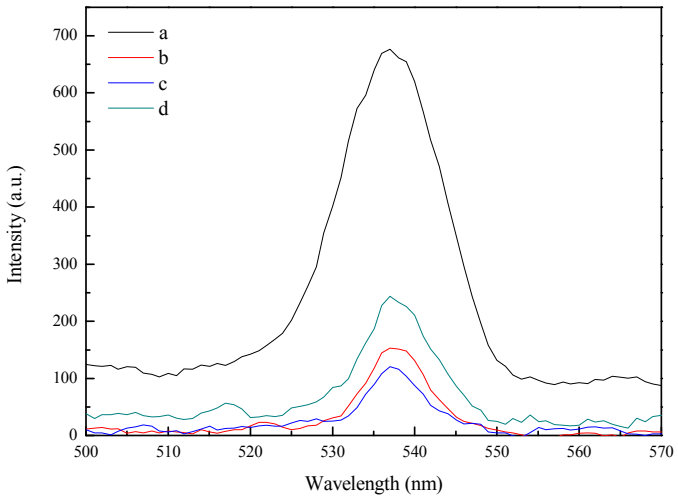

Fig. 5

CrystEngComm Accepted Manuscript

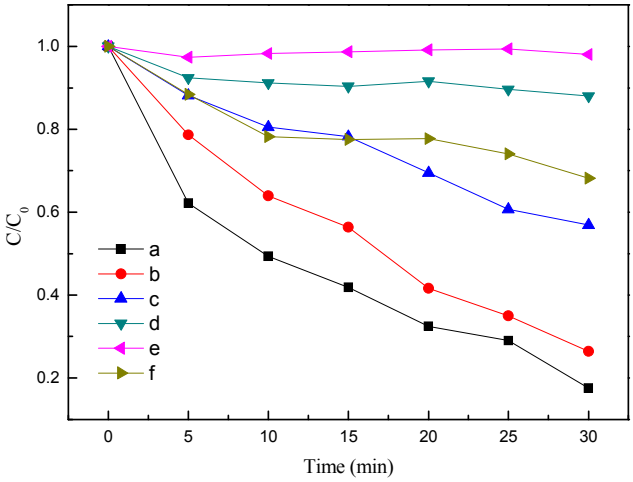

Fig. 6

CrystEngComm Accepted Manuscript

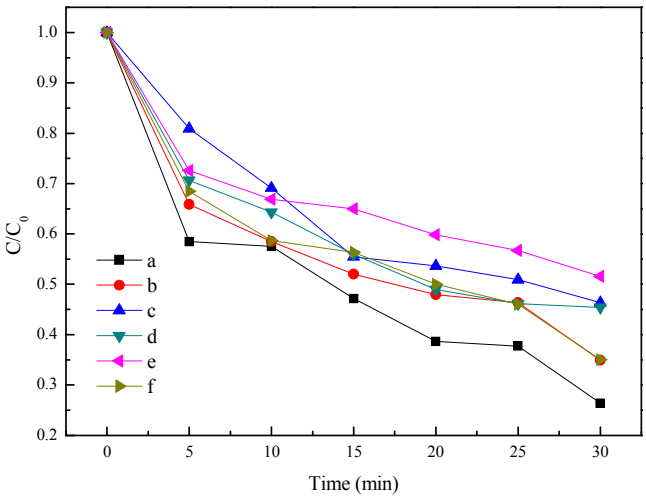

Fig. 7

CrystEngComm Accepted Manuscript

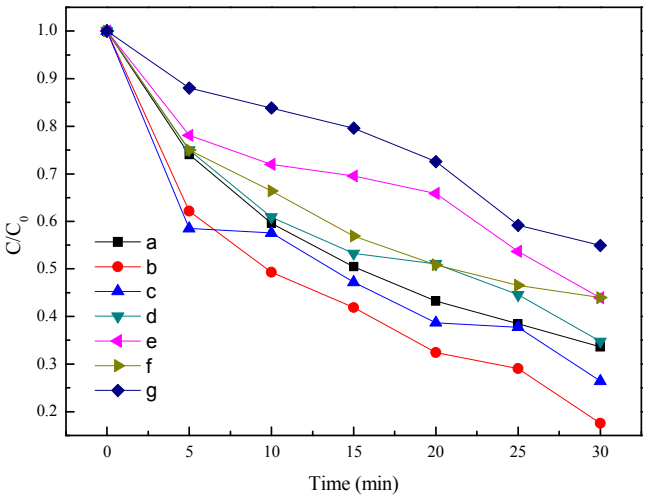

Fig. 8

CrystEngComm Accepted Manuscript

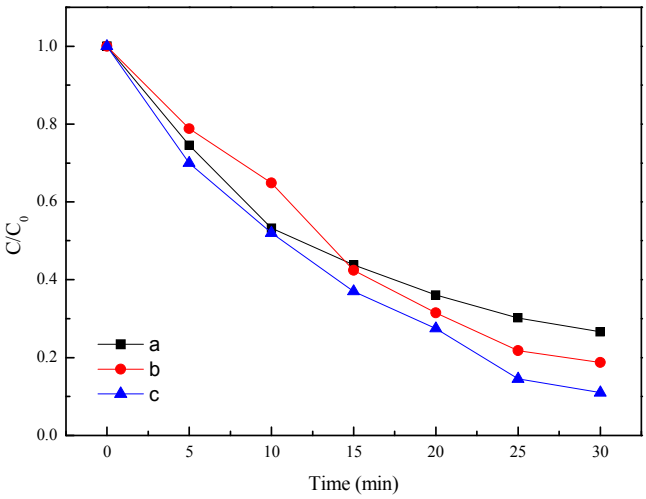

Fig. 9

CrystEngComm Accepted Manuscript

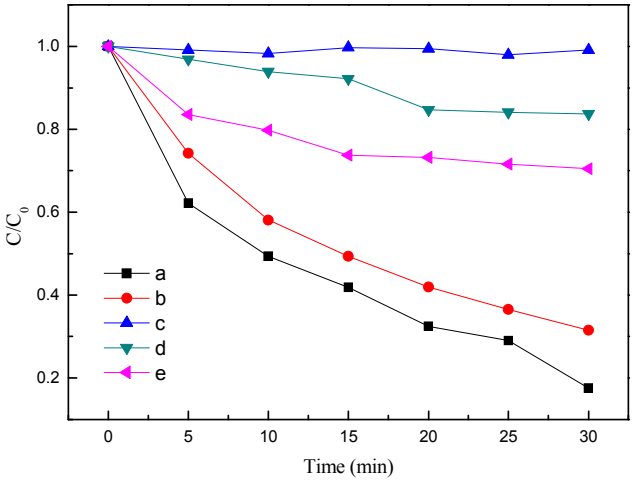

Fig. 10

CrystEngComm Accepted Manuscript

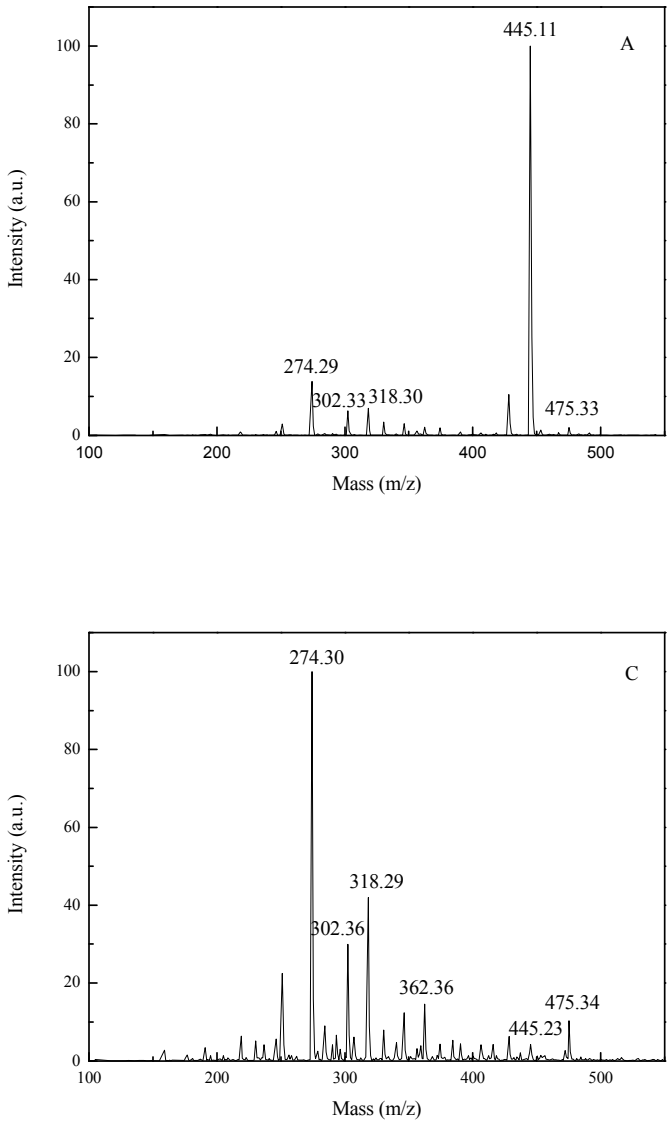

Fig. 11

CrystEngComm Accepted Manuscript

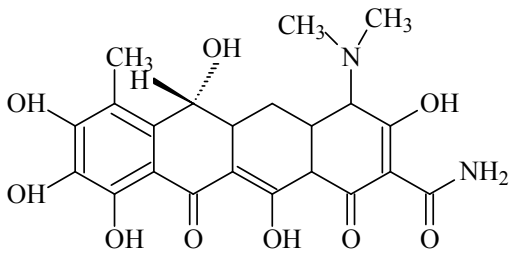

m/z=481

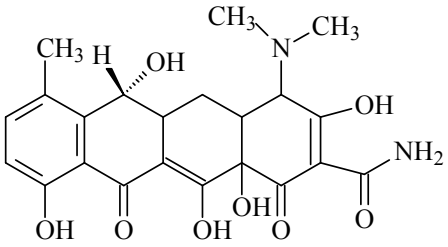

tetracycline hydrochloride

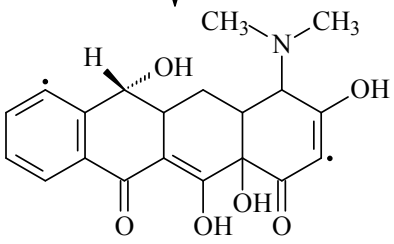

m/z=362

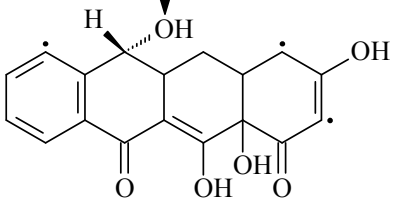

m/z=318

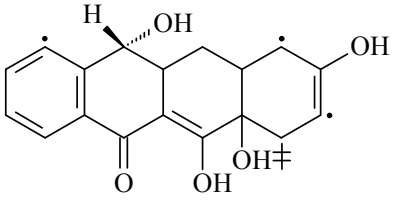

m/z=302

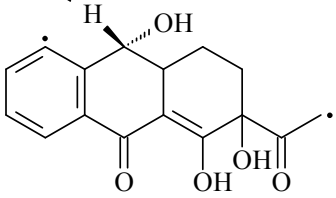

m/z=274

CrystEngComm Accepted Manuscript

Fig. 12

CrystEngComm Accepted Manuscript

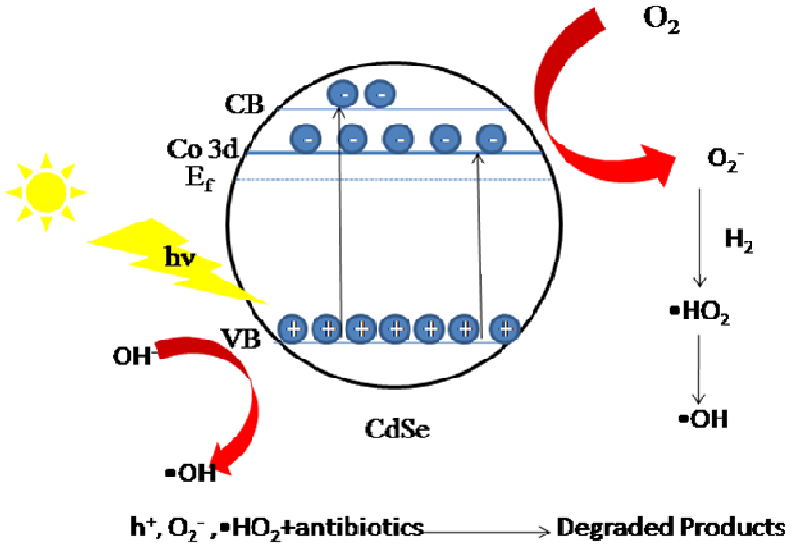

Fig. 13

CrystEngComm Accepted Manuscript

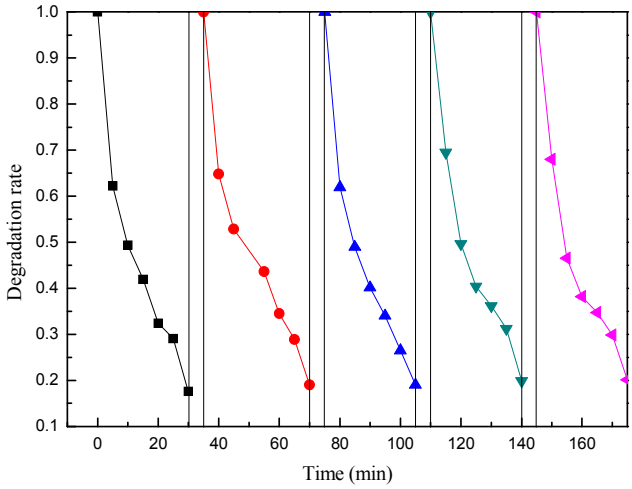

Fig. 14

CrystEngComm Accepted Manuscript

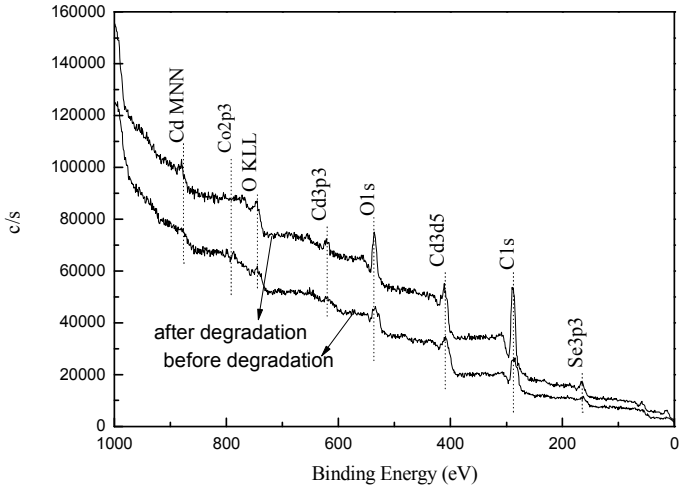

Fig. 15

CrystEngComm Accepted Manuscript

Fig. 1. The XRD patterns of photocatalysts of pure CdSe and 3%Co-4%K/CdSe.

Fig. 2. HRTEM of the 3%Co-4%K/CdSe.

Fig. 3. High resolution XPS spectra of (A) 3%Co-4%K/CdSe, (B) Co 2p, (C) Cd 3d and (D) Se 3d in 3%Co-4%K/CdSe.

Fig. 4. Uv-Vis diffuse reflectance absorption spectra (A) (a) 4%Co-4%K/CdSe (b) 4%Co-4Ca%/CdSe (c) 4%Co-4%Zn/CdSe (d) 4%K-4%Ca/CdSe (e) 4%Zn-4%K/CdSe (f) 4%Zn-4%Ca/CdSe and evaluations of band gap energies by Kubelka – Munk equations (B) of puer CdSe and 4%Co-4%K/CdSe.

Fig. 5. Photoluminescence spectra of (a) pure CdSe (b) 3%Co/CdSe (c) 3%Co-4%K/CdSe and (d) 4%K/CdSe.

Fig. 6. (A) Photocatalytic degradation of tetracycline hydrochloride (a) 3%Co-4%K/CdSe (b) 3%Co/CdSe (c) 4%K/CdSe (d) dark (e) blank and (f) pure CdSe

Fig. 7. Effect of dopants on photodegradation of tetracycline hydrochloride (a) 4%Co-4%K/CdSe (b) 4%Co-4%Ca/CdSe (c) 4%Co-4%Zn/CdSe (d) 4%Zn-4%K/CdSe (e) 4%Zn-4%Ca/CdSe and (f) 4%K-4%Ca/CdSe.

Fig. 8. Effect of proportions of cobalt ions on photodegradation of tetracycline hydrochloride (a) 2%Co-4%K/CdSe (b) 3%Co-4%K/CdSe (c) 4%Co-4%K/CdSe (d) 5%Co-4%K/CdSe (e) 6%Co-4%K/CdSe (f) 7%Co-4%K/CdSe and (g) 8%Co-4%K/CdSe.

Fig. 9. Effect of surfactants on photodegradation of tetracycline hydrochloride (a) SDS (b) PEG 2000 and (c) benzalkonium chloride.

Fig. 10. Effect of electrons and holes on photodegradation of tetracycline hydrochloride (a) 3%Co-4%K/CdSe (b) 3%Co-4%K/CdSe+t-BuOH (c) 3%Co-4%K/CdSe+EDTA-Na (d) 3%Co-4%K/CdSe+methanol and (e) 3%Co-4%K/CdSe+benzoquinone.

Fig. 11. LC chromatograms and m/z of degraded tetracycline hydrochloride (A) tetracycline hydrochloride (B) degradation of tetracycline hydrochloride in 10 min (C) degradation of tetracycline hydrochloride in 20 min and (D) degradation of tetracycline hydrochloride in 30 min.

Fig. 12. The process of degradation $C_{22}H_{24}N_2O_8 \cdot HCl$ with 3%Co-4%K/CdSe.

Fig. 13. Schematic diagram for the mechanism of the degradation tetracycline hydrochloride over 3%Co-4%K/CdSe.

Fig. 14. Repeated experiments of photocatalytic degradation of tetracycline hydrochloride over the 3%Co-4%K/CdSe.

Fig. 15. XPS pattern comparison for 3%Co-4%K/CdSe before tetracycline hydrochloride degradation and after tetracycline hydrochloride degradation for the fifth cycle.

CrystEngComm Accepted Manuscript